

Performance Analysis and Enhancement of WAVE for V2V Non-Safety Applications

Mohammed Amine Togou¹, Lyes Khoukhi, and Abdelhakim Hafid

Abstract—The wireless access for vehicular environment (WAVE) mandates that data packets of non-safety applications are to be sent within WAVE basic service sets (WBSS). These WBSS are to be established on the least congested service channels. WAVE proposes a mechanism to select such channels; yet, owing to vehicles' high mobility, there is high chance of having overlapped WBSS, yielding unsatisfactory performance. Several approaches have been proposed to mitigate this problem. Nevertheless, they are either inefficient or cost-ineffective. In this paper, we propose a novel approach called altruistic service channel selection (ASSCH) that compels vehicles to cooperate in order to select the least congested service channels for vehicle-to-vehicle (V2V) non-safety applications. ASSCH has three phases: 1) identifying the channel's current state (i.e., free or occupied); 2) predicting channels that are likely to be free in the near future; and 3) selecting the least used channel among them. We then propose a stochastic analytical model for the throughput of V2V non-safety applications considering various factors, including the busy channel at zero, discarded by all existing IEEE 802.11p EDCA models. Simulation results demonstrate that ASSCH outperforms existing allocation-based schemes as it incurs low capture delay, low ratio of overlapping WBSS, and high throughput. Simulation results also show that our analytical model closely matches the throughput of EDCA access categories.

Index Terms—EDCA, Markov chains, SCHs, throughput, WAVE, WBSS.

I. INTRODUCTION

WAVE [1] is designed to support intelligent transportation system (ITS) applications. It operates in the dedicated short range communication (DSRC) frequency band (5.8 GHz - 5.925 GHz), which is divided into a 5 MHz guard band and seven 10 MHz channels. One of them is designated as the control channel (CCH) and is exclusively dedicated to transmitting safety and control messages. The remaining six, labeled service channels (SCHs), are used to transfer data

packets of non-safety applications. Coordination between these channels is made possible through the use of the coordinated universal time (UTC), where each second is partitioned into ten synchronization intervals (SI). Each SI consists of one CCH interval (CCI) followed by one SCH interval (SCI). Vehicles have to monitor CCH during CCI to not miss safety messages and can optionally switch to one of SCHs during SCI [1].

WAVE allows for data packets of non-safety applications (i.e., traffic management and infotainment) to be transmitted within WBSS, which can be established by any WAVE device (i.e., RSUs or OBU) [3], [4]. There are two types of WBSS: (1) persistent: announced at every CCI for the entire WBSS lifetime; and (2) non-persistent: announced only once, i.e., when establishing WBSS. [5]. A vehicle having packets to send, labeled *provider*, initiates WBSS by broadcasting Wave Service Advertisement (WSA) message during CCI. WSA contains the provider's identifier, a description of the service provided, and the service channel to be used [6]. When receiving WSA, vehicles may choose to join WBSS. If so, they are labeled *users*; they, along with the provider, switch their transceivers to the advertised SCH at the beginning of the subsequent SCI. The provider then starts transmitting data packets.

WAVE mandates that vehicles shall monitor received WSA messages to keep track of used SCHs in their 1-hop range [7], [8]. This way, providers can select the least congested SCH to establish their WBSS. Yet, when using non-persistent WBSS, this mechanism suffers three major shortcomings: 1) vehicles might end-up using obsolete SCHs information due to WSA collisions; 2) vehicles lack SCHs information within 2-hop range, yielding poor service quality as two providers within carrier sense range may select the same SCH to setup their WBSS (i.e., WBSS overlapping problem); and 3) there is no mechanism for notifying users about WBSS termination, yielding high channel access delay as providers may be denied access to SCHs even if they are available to be used.

To mitigate these issues, we propose ASSCH, a novel channel selection mechanism that has three phases: 1) collecting real-time service channel state information, in 1-hop and 2-hop ranges, via listening for WSAs and compelling vehicles to collaborate; 2) feeding the collected state information to a Markovian model that predicts the state of each service channel in the near future; and 3) selecting the least congested channel, i.e., the least used. To the best of our knowledge, none of the existing schemes have proposed a hybrid approach that uses only one transceiver per vehicle.

Manuscript received November 19, 2016; revised May 7, 2017 and September 17, 2017; accepted September 21, 2017. Date of publication October 30, 2017; date of current version August 1, 2018. The Associate Editor for this paper was C. F. Mecklenbräuer. (*Corresponding author: Mohammed Amine Togou.*)

M. A. Togou is with the Networks Research Laboratory, University of Montreal, Montreal, QC H3T 1N8, Canada, and also with the Environment and Autonomous Networks Laboratory, University of Technology of Troyes, 10004 Troyes, France (e-mail: togoumoh@iro.umontreal.ca).

L. Khoukhi is with the Environment and Autonomous Networks Laboratory, University of Technology of Troyes, 10004 Troyes, France (e-mail: lyes.khoukhi@utt.fr).

A. Hafid is with the Networks Research Laboratory, University of Montreal, Montreal, QC H3T 1N8, Canada (e-mail: ahafid@iro.umontreal.ca).

Color versions of one or more of the figures in this paper are available online at <http://ieeexplore.ieee.org>.

Digital Object Identifier 10.1109/TITS.2017.2758678

Frequency GHz	SCH	SCH	SCH	CCH	SCH	SCH	SCH
	172	174	176	178	180	182	184
	5,86	5,87	5,88	5,89	5,90	5,91	5,92

Fig. 1. DSRC channels: channels 172 and 184 are reserved for public safety applications in the Federal Communication Commission [2].

The rest of the paper is organized as follows. Section II reviews some related work. Section III describes the system model while Section IV presents the service channel selection scheme. Section V describes EDCA throughput analytical model. Section VI presents the simulation results and Section VII concludes the paper.

II. RELATED WORK AND MOTIVATION

Several schemes have been proposed to help alleviate WAVE aforementioned limitations. They are of two types: allocation-based and prediction-based.

Allocation-based schemes [7], [9]–[13] use single or dual transceivers to switch between CCH and SCHs and require vehicles to maintain channel occupancy tables (OCTs), where the state of each SCH is stored. Campolo et al. in [7], proposed CRaSCH, a cooperative reservation scheme for service channels, that requires each provider to maintain SCH state information within its 1-hop and 2-hop ranges. The 2-hop state information is piggybacked into WSAs while the 1-hop information is used to select the least used SCH. In case the WBSS overlapping problem occurs, a channel collision warning (CCW) frame is transmitted to the provider of the last received WSA, urging it to choose another SCH. Similarly, Wang et al. [9] proposed the minimum duration counter (MDC) scheme that piggybacks the occupancy duration of each channel into WSAs so that the least used channels can be selected. References [12] and [13] use the RTS/CTS mechanism to negotiate the use of a common available data channel. Indeed, in [12], a provider chooses a free channel from its OCT and includes it into RTS. When receiving RTS, a user checks if that channel is marked as free in its own OCT. If so, it broadcasts a CTS containing the identifier of the received SCH; otherwise, it broadcasts a rejecting CTS and the whole process is repeated. To make the handshake process quicker, each provider in [13] appends the list of all available channels to RTS. A user compares the list of received available channels with its own OCT. If a match is found, the user replies with CTS containing the identifier of SCH in common. References [10] and [11] use a TDMA scheme to assign slots to vehicles during CCI. This is done via attaching frame information (FI), consisting of the vehicle's identifier and the states of all slots in its 1-hop range, to every transmitted packet over CCH. Finally, Su and Zhang [14] proposed a TDMA cluster-based multichannel MAC where cluster heads (CHs) are responsible for assigning data channels to their respective cluster members.

Prediction-based schemes, on the other hand, require vehicles to be equipped with multiple transceivers to monitor all the channels continuously. They deploy prediction mechanisms to identify channels that are likely to be available

in the near future. For instance, Inage *et al.* [15] created databases to store and provide information regarding geographical and temporal channels availability. Based on this information, the best channel, defined as the channel to be available the longest possible in the movement direction of the vehicle, is selected. Similarly, Chen and Vuyyuru [16] created a spectrum utilization database that keeps track of channels' usage, where the least congested channel is selected. Radunovic *et al.* [17] also created a database to dynamically select the best channel along with the best rate of transmission. The database has two parameters: 1) the number of time periods during which packets were transmitted to a user on a specific channel using a specific rate; and 2) the number of successfully transmitted packets to the same user over the same channel and using the same data rate. The best (channel, rate) pair is selected. Brahmi *et al.* [18] proposed a cluster-based approach for channel selection where cluster members listen to all channels and report their observations to cluster heads (CHs). After aggregating all the observations, CHs decide on the state of each channel in the current time slot and estimate their state in the subsequent time slot using a hidden markov model (HMM). Available channels are assigned by CHs to cluster members based on their message priority (i.e., safety or non-safety). Similarly, Mapar and Chowdhury [19] proposed a framework that requires each vehicle to monitor signal fluctuations in all channels to determine their current states and uses a HMM to identify channels that are likely to be available in the near future. Finally, Boyaci et al. [8] proposed a cross-layer predictive approach to select the best service channel. It consists of collecting energy data at the physical layer and feeding them to the MAC layer. This latter combines the received data with information retrieved from a database containing channel usage history in order to predict the channels' state in the future. The least used channel among the ones to be available is chosen.

Despite their adequate performance, schemes in both categories have limitations. On the one hand, only one busy state is considered, implying that service priority is not supported by allocation-based schemes. Besides, control messages may suffer multiple collisions, especially in dense networks, making the information in OCTs obsolete. This may lead to inaccurate service channel selection. On the other hand, the use of multiple transceivers implies that prediction-based schemes are cost-ineffective (i.e., in 2017, 1 transceiver costs \$335 for new cars and \$233 as aftermarket equipment [20]) and can incur cross-channel interferences. These observations have motivated us to propose ASSCH, a hybrid channel selection mechanism that compels vehicles to cooperate in order to identify the least congested service channel to be used. It requires vehicles to be equipped with single transceivers, uses a stochastic model to capture the different features impacting the channel's choice (e.g., number of providers, service priority, and channel occupancy time), and exploits beacon messages to exchange SCHs state information. The rationale behind choosing beacon messages is twofold: 1) they are transmitted periodically, allowing for SCHs state information to be frequently updated instead of event-driven (i.e., receipt of WSA); and 2) they do not generate

any additional overhead as they are a key component of VANET.

III. SYSTEM MODEL

Our model consists of a multilane highway segment with obstacles (e.g., houses and trees) on both of its sides. Vehicles arrive at the starting point of the highway segment following a Poisson process with an average rate of λ_a and travel with different speeds, uniformly distributed between V_{min} and V_{max} . Beacon messages are generated at a rate of λ_b , enabling vehicles to transmit information regarding speed and location. We adopt the alternating access mode in order to allow for safety and non-safety applications to co-exist and we make use of the FCC amendment [2] regarding DSRC, where only four SCHs are allocated for non-safety applications (see Fig. 1). We set SCH 172 as the default service channel for vehicles that did not join any WBSS.

We are interested in situations where vehicles can provide services for other vehicles in the absence of RSUs. Such a capability is considered especially attractive as an initial deployment strategy to push WAVE market penetration and also for highway scenarios. For example, vehicles with 4G/LTE connections can provide their neighbors (i.e., without 4G/LTE connection) with traffic information and/or weather conditions. Likewise, vehicles can share multimedia files (e.g., music, movies) as well as information regarding services nearby to make passengers' journey more comfortable.

To establish its WBSS, a provider Pv_i , with $i = 0, 1, 2, 3$ denoting its service priority, may request any SCH. Preference will always be given to providers with high priority services. Time is discretized into slots of length T_s . At each slot, a channel can be either free or occupied. Let T_i be the *service time* of Pv_i , defined as the time period between WBSS establishment and termination, and is known only to Pv_i . To make T_i known to all vehicles, we alter its definition. Indeed, we consider T_i as the remaining time until SCH becomes free given that it is currently used by Pv_i . This way, we can model T_i as an exponential distribution with mean value μ_i . The rationale behind this modeling is that T_i is independent of the time the channel has been in use so far, reflecting its memoryless nature.

IV. ALTRUISTICS SCH SELECTION SCHEME

ASSCH has three phases: SCHs state information collection, SCHs future state prediction, and SCH selection. The following subsections present each one of them in details.

A. SCHs State Information Collection

Vehicles maintain Channel State Tables (CSTs) to keep track of channel usage in their vicinities. For each SCH, CSTs have five fields: 1) state, indicating the current occupancy status of the channel. A value of 1 implies that the channel is busy while a value of 0 indicates that the channel is free; 2) provider's identifier; 3) provider's location; 4) provider's priority; and 5) score, representing the utilization ratio of the channel and computed at the end of every SCI.

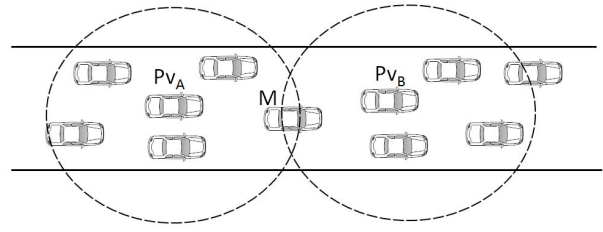


Fig. 2. The monitors selection problem.

Before sending WSA message to setup WBSS, Pv_i collects real-time SCHs state information throughout an entire SI. During CCI, Pv_i listens for broadcasted WSAs in its vicinity and updates its CST accordingly. During SCI, Pv_i requires the cooperation of its neighbors to monitor SCHs. Indeed, when SCI starts, Pv_i switches to SCH 172 and broadcasts *SCH Query (SCHQ)* message to identify the set of neighboring vehicles, S_N , that have not joined any WBSS. When receiving *SCHQ*, every element in S_N replies with a *SCH Response (SCHR)* message, containing its identifier as well as the score of every SCH. Based on received *SCHR* messages, Pv_i chooses *monitors*, i.e., neighbors that will listen to SCHs during the current SCI, based on the following rules:

- If the state of SCH_j is perceived to be free by all vehicles in S_N , monitoring SCH_j is delegated to the farthest neighbor. This helps detecting hidden terminals.
- If otherwise, monitoring SCH_j is delegated to the neighbor with the maximum score for SCH_j .

Once monitors are identified, Pv_i creates and broadcasts the monitoring table (*MT*). Each entry in *MT* contains a monitor identifier as well as its assigned SCH. When receiving *MT*, monitors switch their transceivers to the assigned channels and start listening.

Two providers that are within 2-hop range, as shown in Fig. 2, may select the same vehicle to monitor two different SCHs. Indeed, when the first *MT* is received, assume it is from Pv_A , M will immediately switch to the assigned SCH and starts listening. When Pv_B transmits its *MT*, M will miss it. This will deprive Pv_B from up-to-date information about M 's assigned SCH, leading to inaccurate channel selection decision. To mitigate this issue, we make each monitor broadcasts a small message, labeled *ASSIGNED*, before switching to the assigned SCH. *ASSIGNED* contains the monitor identifier as well as the assigned SCH. It serves two purposes: 1) it acknowledges the receipt of *MT*; and 2) it allows providers to know whether selected monitors are used by other providers.

At the end of SCI, monitors update their CSTs (i.e., state and score of the assigned SCHs) and piggyback them into their beacon messages. When received, vehicles extract the encapsulated CSTs. For each occupied SCH, marked as free in their own CSTs, vehicles use the position field in the received CST to compute their distance to the provider currently using that SCH. In case the distance is smaller than d_{th} , denoting the carrier sense range, they set the state of SCH to busy; otherwise, they keep SCH as free. This is to control the propagation of CSTs, allowing for SCHs spatial reuse without suffering co-channel interferences. According to [21], the

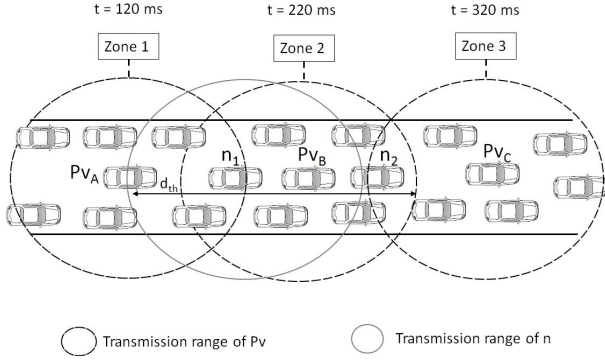


Fig. 3. A sample scenario of three providers setting up their WBSSs at different time instances. The instant t indicates the time at which WSA was transmitted.

average transmission range under the Nakagami propagation model can be expressed as:

$$R_{av} = \left(\frac{1}{\alpha \Gamma(m)} \sum_{i=0}^{m-1} \frac{(m-1)!}{(m-1-i)!} \times \Gamma(m-1-i + \frac{1}{\alpha}) \left(\frac{m P_{th}}{P_i K} \right)^{\frac{1}{\alpha}} \right) \quad (1)$$

where m is the fading factor; $\Gamma(\cdot)$ is the gamma function; α is the path loss exponent; $K = G_t G_r (c/(4\pi f_c))^2$; G_t and G_r are antenna gains of the transmitter and receiver, respectively; c is the speed of light; and $f_c = 5.9$ GHz is the carrier frequency. Hence, d_{th} can be expressed as [21]:

$$d_{th} = \frac{R_{av}}{\rho} \quad \rho \in (0, 1] \quad (2)$$

Fig. 3 shows an example of how CSTs are diffused and updated. After collecting information about SCHs, Pv_A selects SCH_1 and broadcasts its WSA at $t = 120$ ms. When received, vehicles in *zone 1* update SCH_1 entry in their CSTs by setting its state to occupied. They also set the provider identifier, position, and priority to Pv_A 's. At $t = 200$ ms, these vehicles broadcast their beacon messages. When all vehicles in *zone 2*, including Pv_B and n_2 , receive the beacon message from n_1 , they update their CSTs (i.e., SCH_1 entry) accordingly. At $t = 220$ ms, Pv_B broadcasts its WSA with SCH_4 as its selected service channel. Here again, all vehicles in *zone 2* update SCH_4 entry by setting its state to occupied. Then, these vehicles broadcast their beacon messages at $t = 300$ ms. When received, vehicles in *zone 3* compute the distance separating them from Pv_A . Since that distance is greater than d_{th} , they set the state of SCH_1 to free. When Pv_C wants to establish its own WBSS at $t = 320$ ms, it can use available SCHs, including SCH_1 .

B. SCHs Future State Prediction

In this subsection, we predict the state of each channel in the next SCI using the Markovian model depicted in Fig. 4. There are six states $\{S_f, S_h, S_0, S_1, S_2, S_3\}$ describing the channel's state at the end of each SCI. A channel can be free (S_f), occupied by a provider with priority $i = 0, 1, 2, 3$ (S_i), or

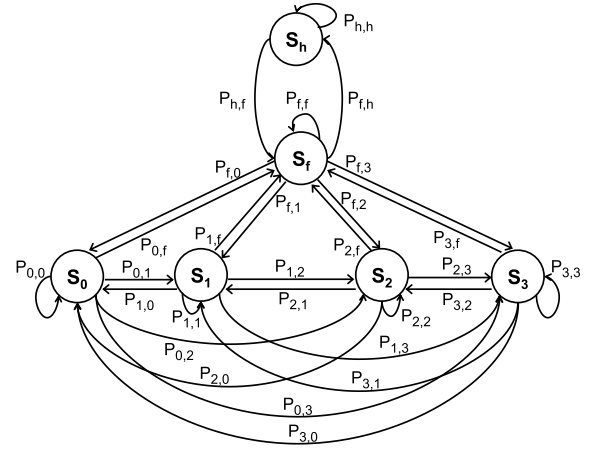


Fig. 4. The Markov chain model for SCHs state prediction in the next SCI.

suffering a hidden terminal problem (S_h). Let p_q^i be the probability of Pv_i requesting a service channel. The transition probabilities of the Markov chain are viewed as conditional probabilities, where $P_{m,j}$ is the probability that the channel will be in state S_m in the next SCI given that it is in state S_j at the end of the current SCI.

Here, we present few elements that are essential to the derivation of the state transition matrix.

- Since vehicles only acquire local information, a provider cannot know the exact number of vehicles within 2-hop range, denoted by n . Using the fact that vehicles arrive to the highway following a Poisson process with rate λ_a , n can be expressed as:

$$n = \frac{4\lambda_a(d_{th} - R_{av})}{V_{min} + V_{max}} \quad (3)$$

- Given that the channel is used by Pv_i in the current SCI, the probability that Pv_i holds the same channel in the next SCI can be expressed as:

$$P_{hold}^i = P(T_i > 1) = e^{-\frac{1}{\mu_i}} \quad (4)$$

- Given that the channel is used by Pv_i in the current SCI, the probability that Pv_i releases the channel at the end of the current SCI is:

$$P_{release}^i = 1 - P_{hold}^i = 1 - e^{-\frac{1}{\mu_i}} \quad (5)$$

- The probability that no provider of priority i requests the channel can be computed as [19]:

$$P_{nrq}^i = e^{-np_q^i} \quad (6)$$

- The probability that at least one provider of priority i requests the channel is expressed as:

$$P_{rq \geq 1}^i = 1 - P_{nrq}^i = 1 - e^{-np_q^i} \quad (7)$$

- The mean value of the service time of providers with different priorities is expressed as:

$$\mu = \sum_{i=0}^3 \mu_i \quad (8)$$

The transition probabilities of the Markov chain, illustrated in Fig. 4, are expressed as follows:

$$P_{f,f} = e^{-n \sum_{i=0}^3 p_q^i} \quad (9)$$

$$P_{f,0} = (1 - e^{-np_q^0}) e^{-n \sum_{i=1}^3 p_q^i} \quad (10)$$

$$P_{f,1} = (1 - e^{-np_q^1}) e^{-n(p_q^2 + p_q^3)} \quad (11)$$

$$P_{f,2} = (1 - e^{-np_q^2}) e^{-np_q^3} \quad (12)$$

$$P_{f,3} = 1 - e^{-np_q^3} \quad (13)$$

$$P_{f,h} = 1 - e^{-n \sum_{i=1}^3 p_q^i} \quad (14)$$

$$P_{0,f} = (1 - e^{-\frac{1}{\mu_0}}) e^{-n \sum_{i=0}^3 p_q^i} \quad (15)$$

$$P_{0,0} = (1 - e^{-np_q^0} + e^{-(np_q^0 + \frac{1}{\mu_0})}) e^{-n \sum_{i=1}^3 p_q^i} \quad (16)$$

$$P_{0,1} = (1 - e^{-\frac{1}{\mu_0}}) (1 - e^{-np_q^1}) e^{-n(p_q^2 + p_q^3)} \quad (17)$$

$$P_{0,2} = (1 - e^{-\frac{1}{\mu_0}}) (1 - e^{-np_q^2}) e^{-np_q^3} \quad (18)$$

$$P_{0,3} = (1 - e^{-\frac{1}{\mu_0}}) (1 - e^{-np_q^3}) \quad (19)$$

$$P_{1,f} = (1 - e^{-\frac{1}{\mu_1}}) e^{-n \sum_{i=1}^3 p_q^i} \quad (20)$$

$$P_{1,0} = (1 - e^{-\frac{1}{\mu_1}}) (1 - e^{-np_q^0}) e^{-n \sum_{i=1}^3 p_q^i} \quad (21)$$

$$P_{1,1} = (1 - e^{-np_q^1} + e^{-(np_q^1 + \frac{1}{\mu_1})}) e^{-n(p_q^2 + p_q^3)} \quad (22)$$

$$P_{1,2} = (1 - e^{-\frac{1}{\mu_1}}) (1 - e^{-np_q^2}) e^{-np_q^3} \quad (23)$$

$$P_{1,3} = (1 - e^{-\frac{1}{\mu_1}}) (1 - e^{-np_q^3}) \quad (24)$$

$$P_{2,f} = (1 - e^{-\frac{1}{\mu_2}}) e^{-n \sum_{i=1}^3 p_q^i} \quad (25)$$

$$P_{2,0} = (1 - e^{-\frac{1}{\mu_2}}) (1 - e^{-np_q^0}) e^{-n \sum_{i=1}^3 p_q^i} \quad (26)$$

$$P_{2,1} = (1 - e^{-\frac{1}{\mu_2}}) (1 - e^{-np_q^1}) e^{-n(p_q^2 + p_q^3)} \quad (27)$$

$$P_{2,2} = (1 - e^{-np_q^2} + e^{-(np_q^2 + \frac{1}{\mu_2})}) e^{-np_q^3} \quad (28)$$

$$P_{2,3} = (1 - e^{-\frac{1}{\mu_2}}) (1 - e^{-np_q^3}) \quad (29)$$

$$P_{3,f} = (1 - e^{-\frac{1}{\mu_3}}) e^{-n \sum_{i=1}^3 p_q^i} \quad (30)$$

$$P_{3,0} = (1 - e^{-\frac{1}{\mu_3}}) (1 - e^{-np_q^0}) e^{-n \sum_{i=1}^3 p_q^i} \quad (31)$$

$$P_{3,1} = (1 - e^{-\frac{1}{\mu_3}}) (1 - e^{-np_q^1}) e^{-n(p_q^2 + p_q^3)} \quad (32)$$

$$P_{3,2} = (1 - e^{-\frac{1}{\mu_3}}) (1 - e^{-np_q^2}) e^{-np_q^3} \quad (33)$$

$$P_{3,3} = 1 - e^{-np_q^3} + e^{-(np_q^3 + \frac{1}{\mu_3})} \quad (34)$$

$$P_{h,h} = e^{-\frac{1}{\mu}} + (1 - e^{-\frac{1}{\mu}}) (1 - e^{-n \sum_{i=0}^3 p_q^i}) \quad (35)$$

$$P_{h,f} = (1 - e^{-\frac{1}{\mu}}) e^{-n \sum_{i=0}^3 p_q^i} \quad (36)$$

After computing the transition probabilities of all possible states, Pv_i predicts the state of each SCH in the next SCI as follows:

$$S_{m,j} = \operatorname{argmax} P_{m,j} \\ m, j \in \{f, h, 0, 1, 2, 3\} \quad (37)$$

C. SCH Selection

The final step is to select the least used SCH on which Pv_i can setup its WBSS. For that, Pv_i classifies SCHs into six sets: S'_f , S'_h , S'_0 , S'_1 , S'_2 , and S'_3 . The subscript of each set denotes the predicted state. When selecting SCH, preference is always given to channels in S'_f . If $S'_f = \{\emptyset\}$, channels in

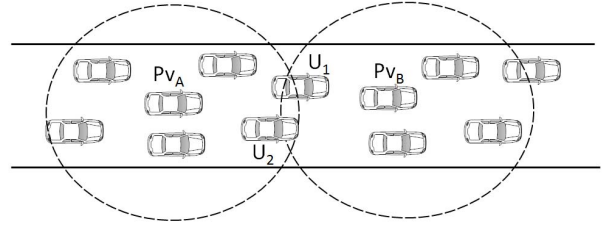


Fig. 5. WBSS Overlapping problem.

S'_j , with $j < i$, are considered. In case $S'_{j < i} = \{\emptyset\}$, we make providers wait till one of the SCHs becomes available. Note that instead of randomly choosing a channel in a set, we select SCH with the lowest score. This is rational since a low score can imply that the current provider has fewer data packets to send. As a result, Pv_i has higher chances of capturing that SCH, lowering therefore the delay to setup its WBSS. Observe also that we did not solicit SCHs in S'_j with $j = i$ and $j > i$ in order to avoid causing collisions to providers with same or higher priority. Observe also that SCHs in S'_h are not considered in order to reduce the possibilities of enduring the hidden terminal problem, thus enhancing the service quality of Pv_i .

It may happen that two providers (Pv_A and Pv_B in Fig. 5), located within 2-hop range, select the same SCH to establish their WBSS (i.e., WBSS overlapping problem), leading to packet collisions. To tackle this problem, ASSCH uses a mechanism similar to the reactive gossiping described in [7]. Indeed, when vehicles U_1 and U_2 in Fig. 5 detect WBSS overlapping problem, they broadcast a warning message, labeled *Overlapping SCH Notification (OSCHN)*. OSCHN contains the SCH in question along with the identifier and the priority of the provider that will keep the channel, selected based on the following rules:

- If Pv_A and Pv_B have different priorities, the provider with the highest priority will keep the channel.
- If Pv_A and Pv_B have the same priority, the first provider to broadcast WSA will keep the channel.

Assume that Pv_A is the one to keep SCH since it has higher priority. To avoid collisions among *OSCHN*, U_1 and U_2 compute a timer before broadcasting *OSCHN*, expressed as follows:

$$T_i = \left(\frac{|d - d'|}{\max(d, d')} \right) + \gamma \quad (38)$$

where d and d' are distances between the current vehicle and Pv_B and Pv_A , respectively and γ is a randomly generated time offset to break the tie when Pv_B and Pv_A are of equal distance to the current vehicle.

Bear in mind that our overlapping SCH notification mechanism is different from the reactive gossiping in two ways. First, ASSCH considers both the providers' priority and WSA generation time when deciding about which provider keeps the channel. Second, unlike the reactive gossiping that relies only on providers to send warning messages, ASSCH impels all vehicles that detect WBSS overlapping problem to get

involved in notifying concerned providers. This makes ASSCH more immune against OSCHN message loss.

V. THROUGHPUT ANALYTICAL MODEL

EDCA defines four access categories (ACs), each having its own parameters, i.e., minimum contention window (CW_{min}), maximum contention window (CW_{max}), and arbitration inter-frame space ($AIFS$). AC_i ($i = 0, 1, 2, 3$) with a packet to send has to sense the channel first. If the channel is sensed idle and stays idle for at least $AIFS_i$, the packet can be transmitted. If the channel is sensed busy, AC_i continues sensing the channel. When it becomes idle and stays idle for $AIFS_i$, AC_i invokes the backoff procedure. To this end, AC_i selects a backoff counter k between 0 and CW_i , where CW_i is set to CW_{min_i} at the beginning. Whenever the channel is sensed idle, k is decremented. Otherwise, k is stopped at its current value (i.e., backoff counter freezing). AC_i resumes decrementing k only when it senses that the channel has been idle for at least $AIFS_i$. When k reaches 0 and the channel is sensed idle, AC_i can transmit its frame. Upon unsuccessful transmission, AC_i will attempt to retransmit the frame. At each retransmission, CW_i is doubled and a new backoff procedure is invoked. When CW_i reaches CW_{max_i} , AC_i uses CW_{max_i} for the upcoming retransmissions. When the retransmission limit r_i is reached, the packet is dropped and CW_i is reset to CW_{min_i} . Note that when k reaches 0 and the channel is sensed busy, AC_i invokes the backoff procedure without changing the value of CW_i (i.e., busy channel at zero). Note also that when a frame is successfully transmitted or dropped, AC_i invokes a new backoff procedure before attempting to transmit the following frame (i.e., post-backoff) [6].

In the literature, few related works (i.e., [22]–[27]) have analyzed the performance of IEEE 802.11p EDCA. Yet, to the best of our knowledge, none of them have considered all the aforementioned factors. For instance, Eichler et al. [22] evaluated the performance of the EDCA mechanism through simulations while considering the collision probability, throughput, and delay. However, no mathematical analysis was provided for the backoff phase. Han et al. [23] proposed an analytical model which lacks the backoff counter freezing and the busy channel at zero mechanisms; in addition, they did not use the same values for AC_i parameters as defined by the IEEE 802.11p standard. Gallardo et al. [24] proposed a Markovian model that was not verified through simulations and does not consider the busy channel at zero mechanism. Likewise, Kaabi et al. [25] presented an analytical model that lacks the busy channel at zero mechanism. Finally, Zheng and Wu [26] proposed a Markovian model to analyze the performance of the EDCA mechanism considering all the aforementioned factors, except the busy channel at zero. In case no packets were queued at the end of the post-backoff phase, AC_i keeps silent. It will contend again for the channel once it has packets to transmit.

In this section, we mathematically analyze the performance of IEEE 802.11p EDCA for V2V non-safety applications. Like most related works, i.e., [23]–[27], we assume that ACs have the same collision probability for different transmissions. We also assume that packet losses are only caused by

TABLE I
NOTATIONS' DEFINITION

Notation	Definition
CW_j^i	Contention window size of AC_i at backoff stage j
m_i	The backoff stage where $CW_m^i = CW_{max}^i$
r_i	Retransmission limit of AC_i
p_b	Probability of the channel sensed busy in a slot
p_{c_i}	Collision probability of AC_i
τ_i	Transmission probability of AC_i
p_{s_i}	Probability of successful transmission for AC_i
T_s	Duration of a time slot
T_L	Transmission time of a packet of size L
T_i	Expected time spent at each state by AC_i

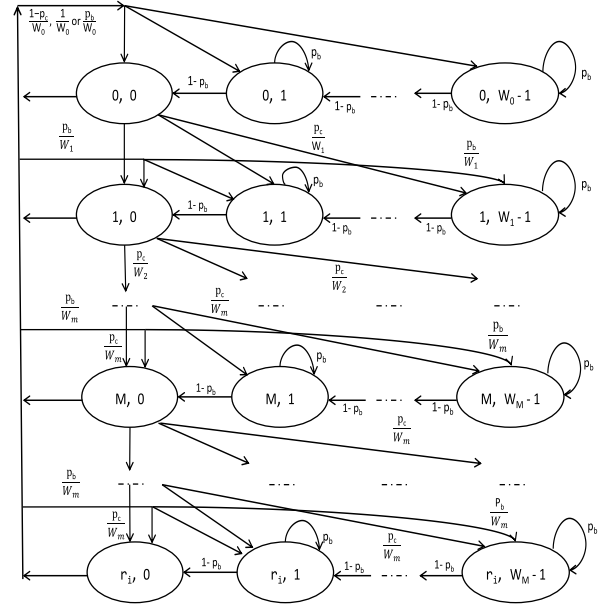


Fig. 6. The Markov chain model for the backoff procedure of an AC.

collisions, excluding channel errors. The notations used in the analysis are summarized in Table I.

Fig. 6 illustrates the 2D Markov chain describing the backoff procedure of AC_i . Each state in the Markov chain is represented by a pair of integers (j, k) , where j denotes the backoff stage while k designates the backoff counter. j is initiated to 0 and is incremented by 1 whenever a collision occurs. When j reaches r_i , the packet is dropped if a collision happens, and j is reset to 0. k is initialized to a value uniformly distributed between $[0, CW_j^i]$ and is decremented by 1 whenever the channel is sensed idle in a slot. CW_j^i is computed as follows:

$$CW_j^i = \begin{cases} CW_{min}^i + 1, & \text{if } j = 0 \\ 2^j CW_0^i, & \text{if } 1 \leq j \leq m_i - 1 \\ CW_{max}^i + 1, & \text{if } m_i \leq j \leq r_i \end{cases} \quad (39)$$

The transition probabilities of the Markov chain in Fig. 6 are expressed as follows:

$$\text{For } 0 < k \leq CW_j^i - 1 \text{ and } 0 \leq j \leq r_i$$

$$P(j, k | j, k) = p_b \quad (40)$$

$$P(j, k - 1 | j, k) = 1 - p_b \quad (41)$$

For $0 \leq k \leq CW_j^i - 1$ and $0 \leq j \leq r_i$

$$P(0, k|j, 0) = \frac{1 - p_{c_i}}{W_0^i} \quad (42)$$

$$P(0, k|r_i, 0) = \frac{1}{W_0^i} \quad (43)$$

$$P(j, k|j-1, 0) = \frac{p_{c_i}}{W_j^i} \quad (44)$$

$$P(j, k|j, 0) = \frac{p_b}{W_j^i} \quad (45)$$

Using the Markov chain in Fig. 6, a transmission occurs when $k = 0$ and the channel is sensed idle. Therefore:

$$\tau_i = (1 - p_b) \sum_{j=0}^{r_i} b(j, 0) \quad (46)$$

where $b(j, 0)$ denotes the stationary probability of state $(j, 0)$. Using Eq. 44, we can express $b(j, 0)$ as follows:

$$b(j, 0) = b(j-1, 0)p_{c_i} \quad \text{for } 1 \leq j \leq r_i \quad (47)$$

By recurring Eq. 47, we have:

$$\sum_{j=0}^{r_i} b(j, 0) = b(0, 0) \sum_{j=0}^{r_i} p_{c_i}^j \quad (48)$$

Since the sum of all states in the Markov chain equals to one, we have:

$$\sum_{j=0}^{r_i} \sum_{k=0}^{W_j^i-1} b(j, k) = 1 \quad (49)$$

By recurring Eqs. 42 - 45 and Eq. 47 for $0 < j \leq r_i$, we obtain:

$$\sum_{k=0}^{W_j^i-1} b(j, k) = \frac{(W_j^i - 1)p_{c_i}^j(1 + p_b)b(0, 0)}{2(1 - p_b)} + b(j, 0) \quad (50)$$

For $j = 0$, and using Eqs. 42 - 45 and Eq. 47, we get:

$$\sum_{k=0}^{W_0^i-1} b(0, k) = \frac{(W_0^i - 1)(1 + p_b)b(0, 0)}{2(1 - p_b)} + b(0, 0) \quad (51)$$

Combining Eq. 50 and Eq. 51, we can compute $b(0, 0)$ as follows:

$$b(0, 0) = \frac{2(1 - p_b)}{1 + p_b} \left[W_0^i \sum_{j=0}^{m-1} 2^j p_{c_i}^j + W_m^i \sum_{j=m}^{r_i} p_{c_i}^j - (1 - 2p_b) \sum_{j=0}^{r_i} p_{c_i}^j \right]^{-1} \quad (52)$$

Hence,

$$\tau_i = \frac{2(1 - p_b)^2 \sum_{j=0}^{r_i} p_{c_i}^j}{1 + p_b} \left[W_0^i \sum_{j=0}^{m-1} 2^j p_{c_i}^j + W_m^i \sum_{j=m}^{r_i} p_{c_i}^j - (1 - 2p_b) \sum_{j=0}^{r_i} p_{c_i}^j \right]^{-1} \quad (53)$$

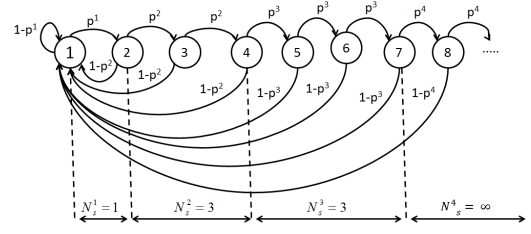


Fig. 7. The 1-D Markov chain for contention phase modeling after a busy period.

Now we need to compute the probability of collision p_{c_i} of AC_i . According to [6], the default values of $AIFS_N$ for AC_0, AC_1, AC_2 and AC_3 on SCHs are 2, 3, 6, and 9, respectively. Given these values, four contention zones ($z_j, j = 1, 2, 3, 4$) can be identified [28]. Different ACs contend in different zones. For example, in z_1 , only AC_0 is allowed to contend for the channel while in z_2 , AC_0 or AC_1 can attempt to transmit. In z_4 , all ACs can attempt to access the medium. Let N_s^j denotes the number of slots in the j^{th} contention zone. The number of slots in each zone is $N_s^1 = 1, N_s^2 = 3, N_s^3 = 3$, and $N_s^4 = \infty$.

To describe the contention phase, we adopt the model presented in [23] and [26]. In this model, the slots involved in the contention phase, after $AIFS_N$, represent the states of the Markov chain (see Fig. 7). The transition from the current state to the next is carried out when the channel is sensed idle. Otherwise, the current state transits to state 1. Hence, the transition probabilities of the Markov chain illustrated in Fig. 7 are expressed as follows:

$$\begin{cases} P(s+1|s) = p^1, & P(1|s) = 1 - p^1 & 1 \leq s \leq N_s^1 \\ P(s+1|s) = p^2, & P(1|s) = 1 - p^2 & s \geq N_s^1 \\ P(s+1|s) = p^3, & P(1|s) = 1 - p^3 & x_1 + 1 \leq s \leq x_2 \\ P(s+1|s) = p^4, & P(1|s) = 1 - p^4 & s \geq x_2 + 1 \end{cases} \quad (54)$$

where $x_1 = N_s^1 + N_s^2, x_2 = x_1 + N_s^3$ and

$$p^j = \prod_{i < j} (1 - \tau_i)^{N_i} \quad j = 1, 2, 3, 4 \quad (55)$$

with N_i designating the number of contending stations having AC_i . Let p_s^s be the stationary probability of state s . Using the Markov chain in Fig. 7, we obtain:

$$p_s^{s+1} = \begin{cases} p_s^s \cdot p^1, & 1 \leq s \leq N_s^1 \\ p_s^s \cdot p^2, & N_s^1 + 1 \leq s \leq N_s^2 \\ p_s^s \cdot p^3, & x_1 + 1 \leq s \leq x_2 \\ p_s^s \cdot p^4, & s \geq x_2 \end{cases} \quad (56)$$

The stationary probability of a zone can be defined as the sum of the stationary probabilities of all states in the

zone [23], [26]. Therefore:

$$\begin{aligned} p_z^1 &= \sum_{s=1}^{N_s^1} p_s^s, & p_z^2 &= \sum_{s=N_s^1+1}^{N_s^2} p_s^s, \\ p_z^3 &= \sum_{s=x_1+1}^x p_s^s, & p_z^4 &= \sum_{s=x_2+1}^{\infty} p_s^s \end{aligned} \quad (57)$$

The collision probability of AC_i in zone z_j (i.e., $p_{c_i}^{z_j}$) is equivalent to the probability that when AC_i has a packet to transmit in a slot, there is at least another $AC_{i'}$ that has a packet to transmit in the same slot. $AC_{i'}$ can have the same priority as AC_i or a different one. Thus, $p_{c_i}^{z_j}$ can be expressed as:

$$p_{c_i}^{z_j} = \begin{cases} 1 - \prod_{i' < i} (1 - \tau_{i'})^{N_{i'}} \cdot \prod_{i \leq i' < j} (1 - \tau_{i'})^{N_{i'}-1}, & i < j \\ 0, & i \geq j \end{cases} \quad (58)$$

Hence, the collision probability of each AC_i can be computed as:

$$p_{c_i} = \frac{\sum_{i \leq j} p_z^j p_{c_i}^{z_i}}{\sum_{i \leq j} p_z^j} \quad (59)$$

Since p_b is the probability that the channel is busy in a slot, it is simply the probability that at least one station is using the channel in that slot.

$$p_b = 1 - \sum_{i=1}^4 p_z^i p^i \quad (60)$$

Let D_i designates the normalized throughput of AC_i , defined as the fraction of time used by AC_i to successfully transmit a frame from the average expected time that AC_i spends in all states. Therefore, we have:

$$D_i = \frac{p_{s_i}^i T_L}{\bar{T}_i} \quad (61)$$

Let $p_{s_i}^{z_j}$ designates the probability of successful transmission of AC_i in zone z_j . $p_{s_i}^{z_j}$ is equivalent to the probability that when AC_i is transmitting in a slot in z_j , no other $AC_{i'}$ has packets to transmit. Again, $AC_{i'}$ can be of the same or different priority than AC_i . Therefore, $p_{s_i}^{z_j}$ can be expressed as:

$$p_{s_i}^{z_j} = \begin{cases} N_i \tau_i \prod_{i \leq i' < j} (1 - \tau_{i'})^{N_{i'}-1} \prod_{i' < i} (1 - \tau_{i'})^{N_{i'}}, & i < j \\ 0, & i \geq j \end{cases} \quad (62)$$

Hence,

$$p_{s_i} = \sum_{j=1}^4 p_z^j p_{s_i}^{z_j} \quad (63)$$

The Markov channel in Fig. 6 shows that \bar{T}_i is not fixed as it depends on the channel's state (i.e., idle or busy). The channel is idle in a slot when no transmission is carried out; therefore, the duration of the idle state is T_s . A busy channel

TABLE II
PARAMETER SETTINGS

Parameter	Value
Data rate	3, 6 Mbps
λ_a	1 vehicle/s
λ_b	10 beacons/s
α, ρ	2, 0.5
P_t	20 mW
P_{th}	3.162e-13 W
μ_2, μ_3 (in seconds)	7, 6
p_q^2, p_q^3	0.01, 0.02
$CW_{min}^0, CW_{min}^1, CW_{min}^2, CW_{min}^3$	3,3,7,15
$CW_{max}^0, CW_{max}^1, CW_{max}^2, CW_{max}^3$	7,7,15,1023
$T_s, SIFS$	13 μ s, 32 μ s
r_i	7

in a slot, however, can be interpreted in two ways: successful transmission or collision. Thus, we have:

$$\bar{T}_i = (1 - p_b)T_s + p_{s_i}T_{suc} + (p_b - p_{s_i})T_c \quad (64)$$

where T_{suc} and T_c are the durations of a successful transmission and a collision, respectively and are expressed as follows:

$$\begin{cases} T_{suc} = AIFS_i + T_h + T_d + SIFS + T_{ACK} + 2\delta \\ T_c = AIFS_i + T_h + T'_d + \delta \end{cases} \quad (65)$$

where T_h , T_d , and T_{ACK} are the transmission times of the header, the payload, and the ACK frame, respectively. T'_d denotes the transmission time of the largest packet involved in the collision and δ represents the propagation delay.

VI. PERFORMANCE EVALUATION AND MODEL VALIDATION

We used OMNET++ [29] along with Veins [30] to implement the different schemes and deployed SUMO [31] to generate realistic mobility traces. The simulation setup is a one directional highway segment of 4000 meters with two lanes. Vehicles' speed is uniformly distributed between 80 and 120 km/h, which is typical for a highway scenario. The Nakagami-m propagation model is used with the fading factor m set to 1.5 for short distances (≤ 80 meters) between transmitters and receivers and decreases to $m = 0.5$ for longer distances (> 80 meters) [29]. The transmitting power is set such that the receiving power within transmission range is the threshold P_{th} as in [21, eq. (2)]. Other parameters are listed in Table II.

A. Performance Evaluation

In this section, we present a simulation-based evaluation of ASSCH and compare it with CRaSCH [7], an allocation-based scheme that is closely related to our work. We also implemented a multi-transceiver ASSCH, called MASSCH, to simulate a prediction-based scheme in order to demonstrate ASSCH high performance. The IEEE 802.11p [6] standard is used as a basis for comparison.

We simulated an application that allows local sharing of two types of files: i) a 5 seconds video file at 20 fps, where each frame is 320×240 with 16.7 million colors; and ii) 30 seconds audio file with 2 channels, 16-bit bit depth, and a sample rate

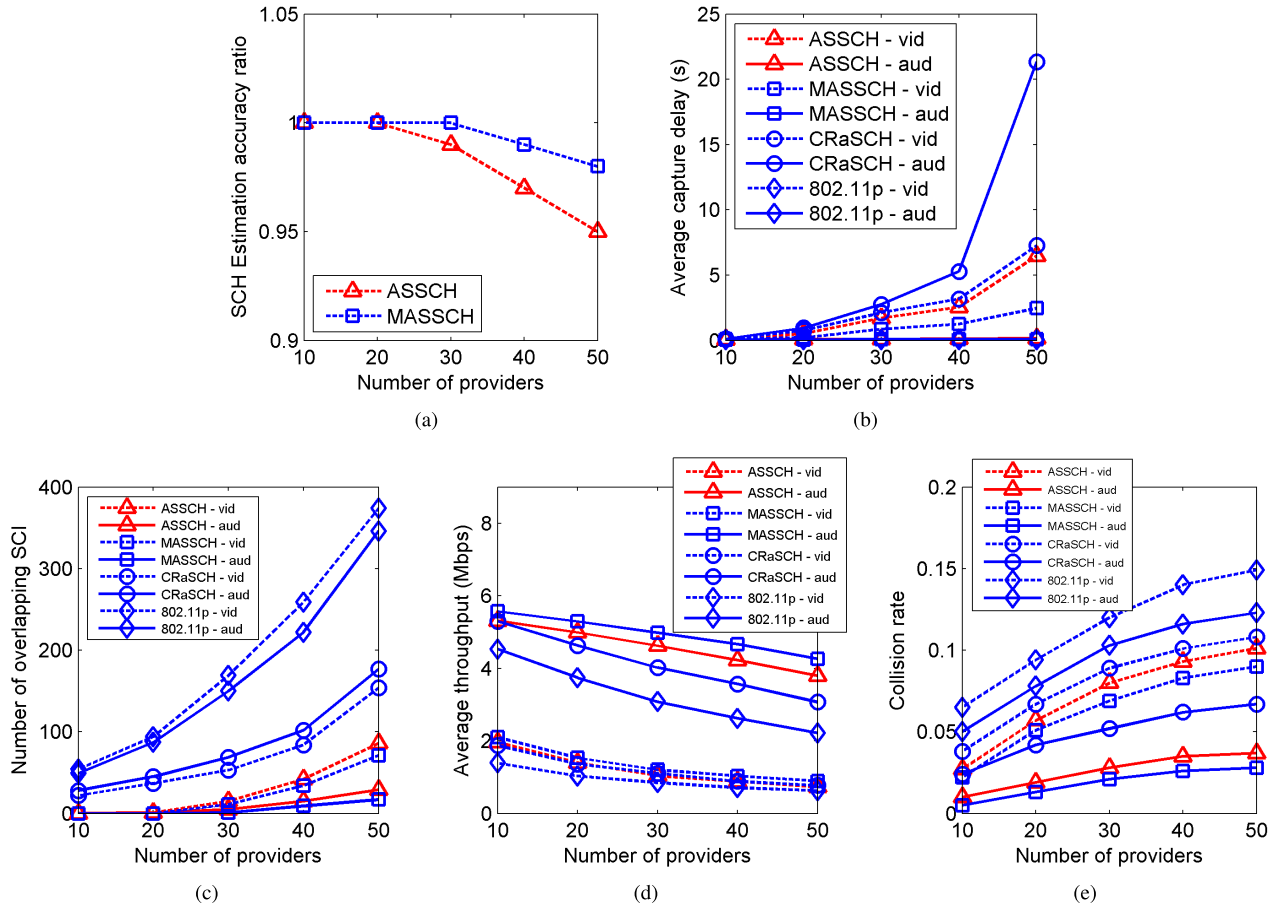


Fig. 8. Simulation results as a function of number of providers: a) Prediction accuracy rate, b) Average capture delay, c) average number of overlapping SCIs, d) average throughput, e) success rate, and f) collision rate.

of 44.1 KHz. When providers reach a specific point in the highway, they randomly choose the type of service to offer (i.e., audio or video), and then trigger the service channel selection process. When receiving WSA, interested vehicles join WBSS. Four metrics were used to assess the performance of the four schemes:

- Prediction accuracy rate: the rate of successfully estimating SCHs state by providers.
- Average capture delay (ACD): the elapsed time between the moment providers send WSA messages and the moment the first data packet is transmitted.
- Overlapping SCI (OVR): the number of SCIs during which the WBSS overlapping problem occurs.
- Average throughput: the amount of data bits transmitted over a time period.

Fig. 8(a) shows the prediction accuracy rate for ASSCH and MASSCH as they are the only schemes to predict SCHs state in the near future. We observe that as the number of providers increases, the prediction accuracy lightly decreases. MASSCH slightly outperforms ASSCH thanks to the use of multiple transceivers, allowing it to continuously monitor SCHs. This offers a better estimation of channels state, making its SCH selection mechanism more accurate. Even though ASSCH only uses one transceiver, its prediction accuracy estimation closely

matches that of MASSCH (i.e., 3% less than MASSCH when the number of providers is set to 50 and 1.4% less on average). The reason is twofold: 1) ASSCH not only uses CSTs, but also compels providers to acquire real-time SCHs state information during SCI via monitors; and 2) ASSCH disseminates SCHs state information using beacon messages, allowing CSTs to be updated periodically, therefore reducing the impact of WSA collisions.

Fig. 8(b) shows ACD variation with the number of providers. We observe that ACD of all schemes increases with the increase of providers' density. IEEE 802.11p generates the lowest delay for both audio and video services. This is because vehicles lack 2-hop visibility, relaxing therefore the spatial SCHs reuse policy. MASSCH outperformed ASSCH and CRaSCH since it uses multiple transceivers. ASSCH experiences lower ACD compared to CRaSCH (e.g., when the number of providers is set to 50, ASSCH incurs ACD that is 11% and 89% lower than CRaSCH for video and audio services, respectively). The reason is threefold: 1) ASSCH gives preference to providers with high priority when selecting SCHs as well as when solving the WBSS overlapping problem. Unlike ASSCH, CRaSCH does not consider service priority, which explains why the video service incurred lower ACD compared to the audio service; 2) ASSCH uses beacon messages,

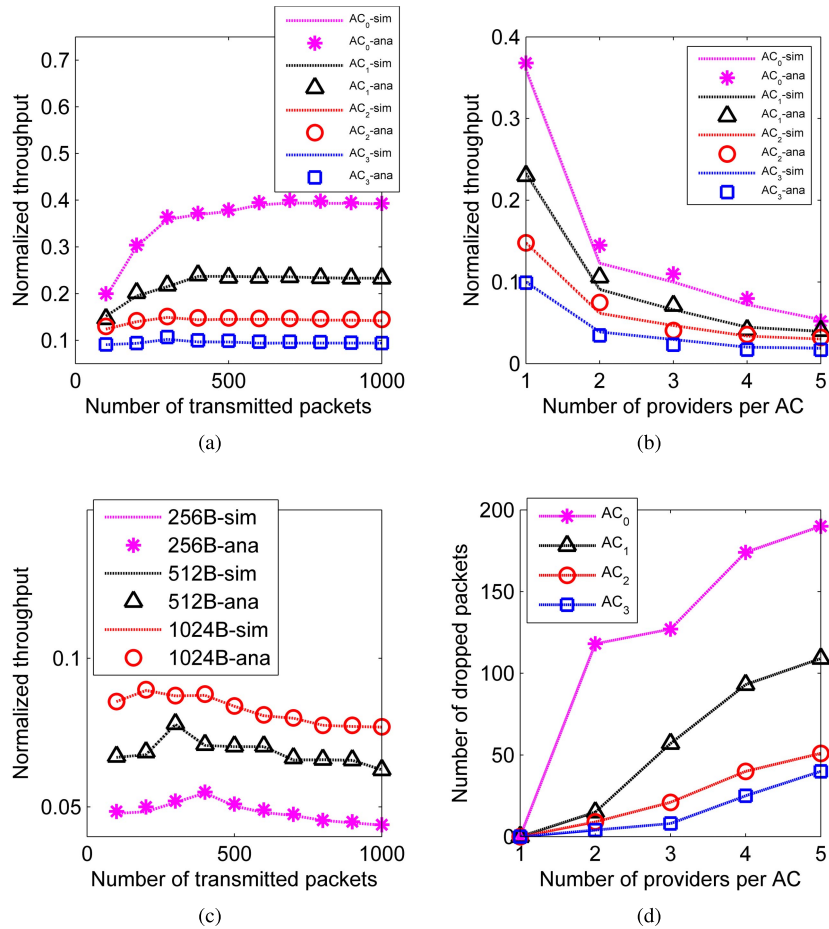


Fig. 9. Simulation results. Normalized throughput of different ACs as a function of a) traffic load (i.e., number of transmitted packets), b) number of providers per AC, and c) packet size. d) Success rate vs. number of transmitted packets.

instead of WSAs, to disseminate CSTs. This helps vehicles maintain up-to-date CSTs even when collisions involving WSA messages occur, allowing for better selection decisions; and 3) ASSCH models the service time as an exponential distribution, allowing vehicles to estimate when WBSS can be terminated. This way, more SCHs can be available for new providers to choose from. Observe that when the number of providers is set to 50, ASSCH provides ACD that is 62% and 34% higher than the one incurred by MASSCH for video and audio services, respectively. This is a tiny price to pay given the cost savings that can be achieved.

Fig. 8(c) shows the overlapping ratio with respect to the number of providers in the network. We observe that OVR for all schemes increases with the number of providers. As expected, MASSCH outperforms all the schemes due to its ability to quickly detect hidden terminals. ASSCH deals better with the overlapping WBSS problem compared to CRaSCH. Indeed, in a network with 50 providers, ASSCH experiences OVR that is 44% and 84% lower than CRaSCH's for video and audio services, respectively. This is because ASSCH compels all vehicles that detect the WBSS overlapping problem to get involved in notifying the conflicting providers. This gives ASSCH a better network visibility, allowing it to closely match the performance of MASSCH (i.e., ASSCH experiences OVR

that is 41% and 17% higher than MASSCH's for video and audio services, respectively, when the number of providers is set to 50). IEEE 802.11p generates the highest OVR as it relies only on received WSAs to keep track of used SCHs. It also lacks a mechanism to address the overlapping WBSS problem.

Figs. 8(d) and 8(e) depict the average throughput and the collision rate (CR) of all schemes as a function of the number of providers. We observe that CR increases as the providers' density increases, implying throughput's drop. Here again, MASSCH outperforms all the schemes thanks to its ability to quickly detect hidden terminals, making it resilient to packet losses. Also, IEEE 802.11p has the worst performance as it lacks 2-hop visibility, making it prone to the hidden terminal problem. ASSCH incurs CR that is 7% and 81% lower than that of CRaSCH for video and audio services, respectively. This is because: 1) like MASSCH, ASSCH can avoid selecting SCHs that suffer from hidden terminal problems thanks to the use of monitors during SCI; 2) giving preference to high priority providers (i.e., audio service) to establish their WBSS first implies efficient SCH utilization. Indeed, SCHs used by high priority providers are not solicited during SCH selection, therefore avoiding unnecessary contention. This yields higher throughput and lower packet loss. Low priority providers, however, might share SCHs with high priority providers.

Consequently, they endure frequent contention, which might increase their collision probability. This explains the low throughput of ASSCH-vid compared to CRaSCH-vid (i.e., CRaSCH allows one WBSS per SCH); and *c*) updating CSTs periodically makes SCHs that were reserved by terminated WBSS quickly available for new providers to exploit. Observe again that ASSCH performed nearly as good as MASSCH since this latter incurs a throughput that is only 14.5% and 3.6% higher than that of ASSCH for audio and video services, respectively, when the number of providers is set to 50.

B. Model Validation

To validate our model, we make providers broadcast WSA messages over CCH, containing SCH 174. Vehicles hearing WSA messages will switch to SCH 174 at the beginning of SCI. At the same time, providers contend for SCH 174 to transmit fixed size UDP packets ($L = 512$ bytes). The data rate is set to 3 Mbps. Fig. 9(a) shows the normalized throughput for the different ACs as a function of traffic load. There are 4 providers, each having packets for a particular AC. All providers are within 1 hop-range, contending to transmit their packets. We observe that the results from the analytical model closely match those of the simulation. We also observe that the normalized throughput has the tendency to stabilize for all ACs as the traffic load increases. This is because ACs have more packets buffered in their queues (i.e., saturation condition), implying that they will continually contend for the channel.

Fig. 9(b) shows the normalized throughput as a function of the number of providers in the network. In this scenario, providers have packets for all ACs and the number of packets to be transmitted is set to 500. Fig. 9(b) shows that simulation results are very close to analytical results. Fig. 9(b) also shows that the normalized throughput of all ACs, AC_0 and AC_1 in particular, quickly decreases when the traffic load increases. The reason is twofold: 1) increasing the number of ACs in the network implies that more ACs will contend for the channel, leading to collisions (i.e., internal and external). Consequently, the probability of transmission τ_i decreases; and 2) increasing the number of ACs can lead to an increase in interferences originated from the hidden terminal areas, reducing therefore the normalized throughput. To support our claim, we computed the number of dropped packets for all ACs; results are shown in Fig. 9(d). We observe that the number of dropped packets increases rapidly for AC_0 and AC_1 as the number of contending ACs increases. For instance, when only one provider has packets for AC_0 , no packet is dropped; however, when five providers have packets for AC_0 , the number of dropped packets reaches 190 (i.e., 38% packet loss).

Finally, Fig. 9(c) depicts the impact of packet size on the normalized throughput for AC_0 . Results of the remaining ACs were not shown for the sake of clarity. Four providers contend for the channel. Each one of them has packets for all ACs. Here again, we observe that simulation results are very close to analytical results. Moreover, as traffic load increases, the normalized throughput of all packet sizes reaches a maximum

value and starts decreasing. This is due to the increase of interfering traffic from hidden nodes and the increase of collisions. Fig. 9(c) also demonstrates that the larger the packet size, the higher is the normalized throughput. This is because large packet sizes allow for the transmission of a high number of data bits compared to low packet sizes (e.g., 256 bytes), reducing therefore the time the channel is perceived as idle.

VII. CONCLUSION

In this paper, we propose ASSCH, a hybrid SCH selection scheme that seeks to enhance the service quality of V2V non-safety applications. ASSCH makes use of WSA messages as well as cooperation among vehicles in order to update CSTs. These CSTs allow providers to select the least used SCH to establish WBSS. We then propose a Markovian analytical model to analyze the performance of IEEE 802.11p EDCA for V2V non-safety applications. Simulation results show that ASSCH outperforms existing allocation-based schemes and performs as good as prediction-based schemes as it allows for quicker access to service channels, handles the overlapping WBSS problem better, and incurs higher throughput as well as high success rate. Therefore, ASSCH can be a good candidate for channel service selection for V2V non-safety applications, particularly during the initial deployment of VANET, since multi-transceiver vehicles might not be widely popular [4].

REFERENCES

- [1] *IEEE Standard for Wireless Access in Vehicular Environments (WAVE)—Multi-Channel Operation*, IEEE Standard 1609.4, Feb. 2011.
- [2] *Amendment of the Commission's Rules Regarding Dedicated Short-Range Communication Services in the 5.850-5.925 GHz Band (5.9 GHz Band)*, document FCC 06-110, FCC Memorandum Opinion Order, Jul. 2006.
- [3] J. B. Kenney, "Dedicated short-range communications (DSRC) standards in the United States," *Proc. IEEE*, vol. 99, no. 7, pp. 1162–1182, Jul. 2011.
- [4] Y. L. Morgan, "Notes on dsrc and wave standards suite: Its architecture, design, and characteristics," *Commun. Surv. Tuts.*, vol. 12, no. 4, pp. 504–518, Oct. 2010.
- [5] C.-M. Huang and C. Yuh-Shyan, *Telematics Communication Technologies and Vehicular Networks: Wireless Architectures and Applications*. Hershey, PA, USA: IGI Global, 2010.
- [6] *Wireless LAN Medium Access Control (MAC) and Physical Layer (PHY) Specifications*, IEEE Standard 802.11-2012, 2012.
- [7] C. Campolo, A. Cortese, and A. Molinaro, "CRaSCH: A cooperative scheme for service channel reservation in 802.11p/WAVE vehicular ad hoc networks," in *Proc. Int. Conf. Ultra Mod. Telecommun. Workshops (ICUMT)*, Oct. 2009, pp. 1–8.
- [8] A. Boyaci, A. H. Zaim, and C. Sönmez, "A cross-layer adaptive channel selection mechanism for IEEE 802.11p suite," *EURASIP J. Wireless Commun. Netw.*, vol. 1, p. 214, Dec. 2015.
- [9] K.-L. Wang, T.-P. Wang, and C.-C. Tseng, "A fair scheme for multi-channel selection in vehicular wireless networks," *Wireless Pers. Commun.*, vol. 73, no. 3, pp. 1049–1065, 2013.
- [10] N. Lu, X. Wang, P. Wang, P. Lai, and F. Liu, "A distributed reliable multi-channel mac protocol for vehicular ad hoc networks," in *Proc. IEEE Intell. Vehicles Symp.*, Jun. 2009, pp. 1078–1082.
- [11] N. Lu, Y. Ji, F. Liu, and X. Wang, "A dedicated multi-channel MAC protocol design for VANET with adaptive broadcasting," in *Proc. IEEE WCNC*, Apr. 2010, pp. 1–6.
- [12] J. Shi, T. Salonidis, and E. W. Knightly, "Starvation mitigation through multi-channel coordination in CSMA multi-hop wireless networks," in *Proc. 7th ACM Int. Symp. Mobile Ad Hoc Netw. Comput. (MobiHoc)*, 2006, pp. 214–225.
- [13] C. Han, M. Dianati, R. Tafazolli, and R. Kernchen, "Asynchronous multi-channel mac for vehicular ad hoc networks," in *Proc. IEEE Veh. Netw. Conf. (VNC)*, Nov. 2011, pp. 109–115.

- [14] H. Su and X. Zhang, "Clustering-based multichannel mac protocols for qos provisionings over vehicular ad hoc networks," *IEEE Trans. Veh. Technol.*, vol. 56, no. 6, pp. 3309–3323, Nov. 2007.
- [15] K. Inage, S. Lee, T. Fujii, and O. Altintas, "White space vectors for channel selection in vehicular cognitive networks," in *Proc. IEEE Veh. Netw. Conf. (VNC)*, Nov. 2011, pp. 55–61.
- [16] S. Chen and R. Vuyyuru, "Dynamic channel selection for wireless mobile ad hoc networks: Adaptation and learning," in *Proc. IEEE 9th Int. Conf. Wireless Mobile Comput., Netw. Commun. (WiMob)*, Oct. 2013, pp. 75–82.
- [17] B. Radunovic, A. Proutiere, D. Gunawardena, and P. Key, "Dynamic channel, rate selection and scheduling for white spaces," in *Proc. 7th Conf. Emerg. Netw. Experim. Technol. (CoNEXT)*, 2011, pp. 2-1–2-12.
- [18] I. H. Brahmi, S. Djahel, and Y. Ghamri-Doudane, "A hidden Markov model based scheme for efficient and fast dissemination of safety messages in VANETs," in *Proc. IEEE Global Commun. Conf. (GLOBECOM)*, Dec. 2012, pp. 177–182.
- [19] F. Mapar and K. Chowdhury, "Predictive decision-making for vehicular cognitive radio networks through hidden Markov models," in *Proc. IEEE Int. Conf. Commun. (ICC)*, Jun. 2014, pp. 1537–1542.
- [20] U. D. of Transportation Office of the Assistant Secretary for Research and Technology. *Costs and Outlook of On-Board Equipment for Connected Vehicles*. Accessed: Jan. 27, 2017. <http://www.itscosts.its.dot.gov/its/benecost.nsf/>
- [21] K. A. Hafeez, L. Zhao, B. Ma, and J. W. Mark, "Performance analysis and enhancement of the DSRC for VANET's safety applications," *IEEE Trans. Veh. Technol.*, vol. 62, no. 7, pp. 3069–3083, Sep. 2013.
- [22] S. Eichler, "Performance evaluation of the IEEE 802.11p wave communication standard," in *Proc. IEEE 66th Veh. Technol. Conf. (VTC-Fall)*, Sep. 2007, pp. 2199–2203.
- [23] C. Han, M. Dianati, R. Tafazolli, R. Kernchen, and X. Shen, "Analytical study of the IEEE 802.11p MAC sublayer in vehicular networks," *IEEE Trans. Intell. Transp. Syst.*, vol. 13, no. 2, pp. 873–886, Jun. 2012.
- [24] J. Gallardo, D. Makrakis, and H. Mouftah, "Performance analysis of the EDCA medium access mechanism over the control channel of an IEEE 802.11p WAVE vehicular network," in *Proc. IEEE Int. Conf. Commun. (ICC)*, Jun. 2009, pp. 1–6.
- [25] F. Kaabi, P. Cataldi, F. Filali, and C. Bonnet, "Performance analysis of IEEE 802.11p control channel," in *Proc. 6th Int. Conf. Mobile Ad-hoc Sensor Netw. (MSN)*, Dec. 2010, pp. 211–214.
- [26] J. Zheng and Q. Wu, "Performance modeling and analysis of the IEEE 802.11p EDCA mechanism for VANET," *IEEE Trans. Veh. Technol.*, vol. 65, no. 4, pp. 2673–2687, Apr. 2015.
- [27] V. P. Harigovindan, A. V. Babu, and L. Jacob, "Tuning transmission opportunity (txop) limits for providing bit-based fairness in IEEE 802.11p V2I networks," in *Proc. Int. Conf. Adv. Comput., Commun. Informat. (ICACCI)*, Aug. 2012, pp. 248–254.
- [28] M. A. Togou, L. Khoukhi, and A. Hafid, "IEEE 802.11p EDCA performance analysis for vehicle-to-vehicle infotainment applications," in *Proc. IEEE Int. Conf. Commun. (ICC)*, May 2017, pp. 1–6.
- [29] O. Ltd. *OMNeT++ Discrete Event Simulator*. Accessed: Apr. 23, 2016. [Online]. Available: <https://omnetpp.org/>
- [30] C. Sommer. *Veins—Vehicles in Network Simulation*. Accessed: Apr. 23, 2016. [Online]. Available: <http://veins.car2x.org/>
- [31] R. Hillbrich. *SUMO—Simulation of Urban Mobility*. Accessed: Apr. 23, 2016. [Online]. Available: <http://www.dlr.de>



Mohammed Amine Togou received the B.S. and M.S. degrees in computer science and computer networks from Al Akhawayn University, Ifrane, Morocco, in 2009 and 2011, and the Ph.D. degree in computer science from the University of Montreal, Montreal, QC, Canada, and the University of Technology of Troyes, Troyes, France, in 2017. He is a Research Fellow with the University of Montreal. His current research interests include connected vehicles, cloud computing, machine learning, smart cities, and cybersecurity.



Lyes Khoukhi received the Ph.D. degree in electrical and computer engineering from the University of Sherbrooke, Sherbrooke, QC, Canada, in 2006. In 2008, he was a Researcher with the Department of Computer Science and Operations Research, University of Montreal, Montreal, QC, Canada. Since 2009, he has been an Assistant Professor with the University of Technology of Troyes, Troyes, France. He has authored or co-authored over 60 publications in reputable journals, conferences, and workshops in the area of resources management in mobile and wireless networks. His research interests include mobile and wireless networks, resources management, QoS and multimedia, and communication protocols. He has participated as a General Chair, Session Chair, or Program Committee Member of many conferences.



Abdelhakim Hafid is a Full Professor with the University of Montreal, where he founded the Network Research Laboratory in 2005. He is also a Research Fellow with CIRRELT, Interuniversity Research Center on Enterprise Networks, Logistics and Transportation. Prior to joining the University of Montreal, he spent several years, as a Senior Research Scientist, with Telcordia Technologies (formerly Bell Communications Research), NJ, USA, where he was involved in major research projects on the management of next generation networks, including wireless and optical networks. He was also an Assistant Professor with Western University, Canada, the Research Director of the Advance Communication Engineering Center (venture established by UWO, Bell Canada, and Bay Networks), Canada, a Researcher with CRIM, Canada, the Visiting Scientist with GMD-Fokus, Berlin, Germany, and a Visiting Professor with the University of Evry, France. He has extensive academic and industrial research experience in the area of the management of next generation networks, including wireless and optical networks, QoS management, distributed multimedia systems, and communication protocols.